Bioconjugate Chemistry

Communication

pubs.acs.org/bc

Glycan-Functionalized Fluorescent Chitin Nanocrystals for Biorecognition Applications

Juan Zhou,[†] Núria Butchosa,[‡] H. Surangi N. Jayawardena,[§] Qi Zhou,[∥,⊥] Mingdi Yan,*[,†,§] and Olof Ramström*[,†]

[†]Department of Chemistry, KTH - Royal Institute of Technology, S-10044 Stockholm, Sweden

[‡]Department of Fiber and Polymer Technology, KTH - Royal Institute of Technology, S-1004 Stockholm, Sweden

[§]Department of Chemistry, University of Massachusetts Lowell, 1 University Avenue, Lowell, Massachusetts 01854, United States

[∥]Wallenberg Wood Science Center, KTH - Royal Institute of Technology, SE-10044 Stockholm, Sweden

[⊥]School of Biotechnology, KTH - Royal Institute of Technology, AlbaNova University Center, S-10691 Stockholm, Sweden

Supporting Information

ABSTRACT: A new platform based on chitin nanocrystals has been developed for biorecognition applications. TEMPO-oxidized chitin nanocrystals (TCNs) were labeled with a fluorescent imidazoisoquinolinone dye, and simultaneously conjugated with carbohydrate ligands, resulting in dually functionalized TCNs. The biorecognition properties of the nanocrystals were probed with lectins and bacteria, resulting in selective interactions with their corresponding cognate carbohydrate-binding proteins, as visualized by optical, fluorescence, STEM, and TEM imaging. This represents a new approach to multifunctional nanomaterials based on naturally occurring polymers, holding high potential for biomedical applications.

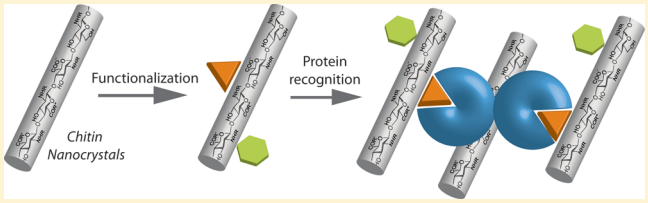

INTRODUCTION

Chitin, the second most plenteous polysaccharide after cellulose, is a linear polysaccharide containing β-(1→4)-2-acetamido-2-deoxy-D-glucopyranose repeating units.[1−7] Chitin is becoming an increasingly important material due to its abundance in nature, as well as its unique properties such as low density, biodegradability, and biocompatibility. However, chitin is insoluble in common solvents, which makes the material difficult to process and limits its uses in practical applications. To overcome this challenge for broader applications, methods have been developed to isolate nanoparticles from chitin.[8] For example, when water-insoluble chitin is subjected to treatment with TEMPO/NaBr/NaClO at pH 10 followed by mechanical disintegration, a stable colloidal aqueous suspension of chitin nanocrystals is produced owing to selective oxidation of the C6 primary hydroxyl groups.[9]

The nanoscale dimension, in the case of chitin characterized by high surface area, unique morphology, and mechanical strength,[8] makes these materials highly attractive as fiber reinforcement agents in tissue engineering and in nanocomposites with natural and synthetic polymers.[10] As a nanomaterial derived from abundant natural sources, chitin nanocrystals would make an excellent platform for biomedical applications, for example, in imaging,[11] sensing,[12] and theranostics.[8] This has been addressed in this study, where TCNs were simultaneously labeled with a fluorescent dye and conjugated with specific carbohydrate ligands. The biorecognition properties of the resulting dually functionalized TCNs were subsequently studied by evaluating the binding of the fluorescent TCNs with cognate lectins and bacteria. To the best of our knowledge, this is the first report on fluorescent chitin nanocrystals for imaging and bioanalysis.

RESULTS AND DISCUSSION

TCNs were prepared from α-chitin of shrimp shells following a previously reported protocol with slight modifications (Scheme 1; see Supporting Information for experimental details),[13,14] yielding individual nanocrystals having a coniferous shape of 6 ± 2 nm in width and 250 ± 110 nm in length (Figure 1a,b).

The X-ray diffraction spectrum of the TCNs showed peaks at 9.2°, 19.3°, 20.9°, and 23.3°, a typical diffraction pattern for TEMPO-oxidized chitins (Figure S1). The total carboxylate content of the TCNs samples was 0.57 mmol/g as determined by conductometric titrations (Figure S2), corresponding to a degree of carboxylation of 0.16.

The TCNs were subsequently labeled with a fluorescent dye (**2**) and a carbohydrate ligand (**5**), an α-D-mannopyranoside (Man) carrying a 2-(2-(2-aminoethoxy)ethoxy)ethanol aglycon chain. The dye, 4-(2-aminoethylamino)-7*H*-benz[*de*]imidazo-[2,1-*a*]isoquinolin-7-one (**2**), gives greenish yellow fluorescence (Figure S3) and was chosen due to its fastness properties and high relative fluorescence intensity.[15,16] Activation of the

Received: January 3, 2014
Revised: March 11, 2014
Published: March 13, 2014

   dx.doi.org/10.1021/bc500004c | *Bioconjugate Chem.* 2014, 25, 640−643

Scheme 1. Chitin Nanocrystal Formation via TEMPO-Mediated Oxidation of Chitin

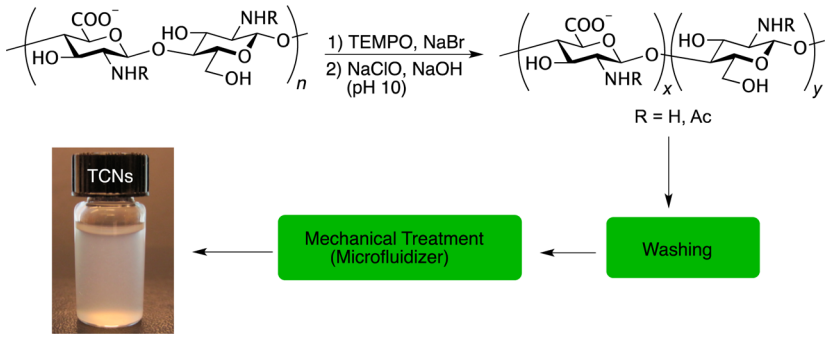

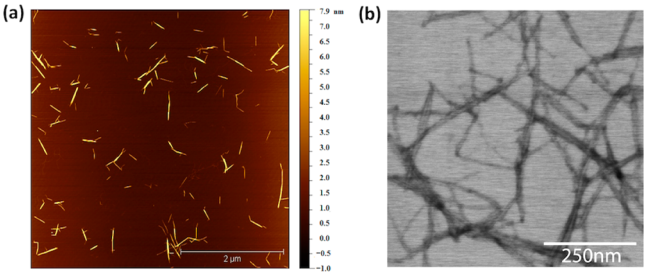

Figure 1. (a) AFM and (b) scanning transmission electron microscopy (STEM) images of TCNs.

carboxyl groups in TCNs with EDC and NHS followed by conjugation with the dye **2** and Man derivative **5** yielded the dually functionalized nanocrystal **TCN-dye-Man** (Scheme 2; see Supporting Information for experimental details). The carboxyl groups in TCN were functionalized in high yield, as evidenced by the disappearance of the carboxyl absorption band around 1740 cm^{-1} in the FTIR spectrum (Figure S4).

Scheme 2. Synthesis of Dually Functionalized TCNs

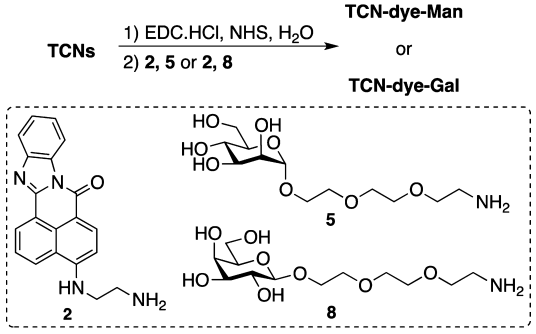

The bioactivity of **TCN-dye-Man** was subsequently tested by treating the nanocrystals with the lectin concanavalin A (Con A), a carbohydrate-binding protein that has specific affinity toward α-D-mannopyranosides,[17−20] and, to a lesser extent, to α-D-glucopyranoside-containing ligands (see Supporting Information for experimental details).[21−23] Con A exists as a tetramer at pH 7.2, thus enabling potential cross-linking of the multivalent **TCN-dye-Man** and causing aggregation of the nanocrystals. Indeed, when Con A was added to **TCN-dye-Man**, aggregates were observed in less than 5 min (Figure 2a II), whereas without Con A, the nanocrystals stayed suspended in the solution (Figure 2a I). This was further confirmed by STEM where the aggregation was visible in the **TCN-dye-Man** sample treated with Con A (Figure 3a) as compared to the sample without Con A (Figure 1b). In a control experiment, **TCN-dye-Man** was incubated with soybean agglutinin (SBA),[24−26] a lectin that primarily binds to 2-acetamido-2-deoxy-β-D-galactopyranosides, and to a lesser extent to β-D-galactopyranoside-containing carbohydrates.[26] No precipitation was observed and the nanocrystal solution remained homogeneous for over 40 min (Figure 2a III). The fluorescence spectrum of the **TCN-dye-Man** solution after treating with Con A for one hour showed a significantly reduced emission intensity, while only a slight decrease was observed when **TCN-dye-Man** was treated with SBA (Figure 2c), likely due to nonspecific adsorption of SBA to the nanocrystals.[27,28]

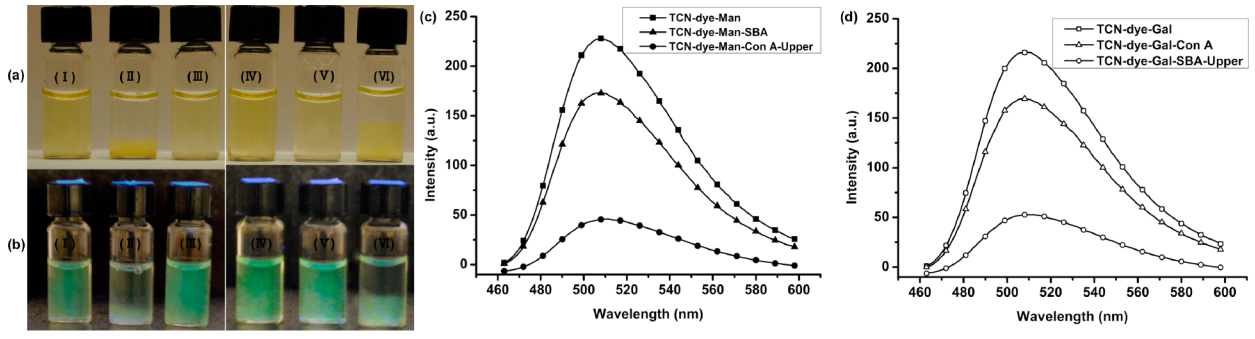

Figure 2. TCN-dye-Man and **TCN-dye-Gal** in HEPES buffer (pH 7.2) under (a) visible light and (b) UV illumination: **TCN-dye-Man** (I), **TCN-dye-Man** incubated with Con A (II), **TCN-dye-Man** incubated with SBA (III), **TCN-dye-Gal** (IV), **TCN-dye-Gal** incubated with Con A (V), and **TCN-dye-Gal** incubated with SBA (VI). (c) Emission spectra of **TCN-dye-Man** (■), **TCN-dye-Man** with SBA (▲), and **TCN-dye-Man** with Con A (●). (d) Emission spectra of **TCN-dye-Gal** (□), **TCN-dye-Gal** with SBA (○) and **TCN-dye-Gal** with Con A (Δ). λ_{ex} = 450 nm, λ_{em} = 512 nm.

dx.doi.org/10.1021/bc500004c | *Bioconjugate Chem.* 2014, 25, 640−643

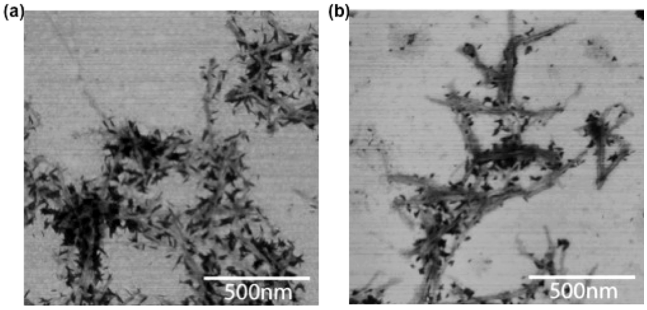

Figure 3. STEM images of (a) **TCN-dye-Man** after treating with Con A and (b) **TCN-dye-Gal** after treating with SBA.

To further confirm the binding affinity and specificity of glycan-functionalized TCNs, β-D-galactopyranoside (**8**)[13,14] was conjugated to TCNs following the same procedure as for mannoside **5** to yield **TCN-dye-Gal** (Scheme 2; see Supporting Information for experimental details). The biorecognition properties of the resulting nanocrystals were then evaluated using Con A and SBA, respectively. Agglomeration was observed in the sample incubated with SBA (Figure 2a VI). Compared to the case where **TCN-dye-Man** was treated with Con A, the formation of agglomerates was in this case less obvious. This is likely due to the weaker binding affinity between SBA and β-D-galactopyranosides (K_a for methyl β-D-galactopyranoside = 5.5×10^2 M^{-1})[29] than that between Con A and α-D-mannopyranosides (K_a for methyl α-D-mannopyranoside is 8.2×10^3 M^{-1}).[30,31] This was further supported by STEM, which showed stacked chitin nanocrystals (Figure 3b) instead of the dense agglomeration in the case of **TCN-dye-Man**/Con A. On the other hand, the samples remained homogeneous in the absence of SBA (Figure 2a IV), or when incubated with Con A (Figure 2a V). Similar to **TCN-dye-Man**, a drastic decrease in the fluorescence intensity occurred after treatment of the **TCN-dye-Gal** solution with SBA for one hour (Figure 2d). The sample treated with Con A showed a slight intensity decrease during the same time (Figure 2d), likely due to nonspecific protein adsorption on the nanocrystals.

The biorecognition properties of the dually functionalized chitin nanocrystals were further investigated in bacteria binding studies (see Supporting Information for experimental details). Two strains of *E. coli* were probed: ORN 178 and ORN 208, the first of which expressing the α-D-mannoside selective FimH lectin on type 1 pili, whereas the second is devoid of this expression.[32−34] When **TCN-dye-Man** was treated with ORN 178, binding of nanocrystals was observed at the surface of the ORN 178 cells as shown in both the TEM image (Figure 4a) and the confocal fluorescence image (Figure 4c), indicating the interactions between the mannose ligands of **TCN-dye-Man** and the FimH lectin on ORN 178. In contrast, almost no nanocrystals were detected at the surface of ORN 208 cells after treating with **TCN-dye-Man** (Figure 4b,d).

In summary, we have developed a simple protocol for the synthesis of chitin nanocrystals conjugated with both a fluorescent dye and carbohydrate ligand. To demonstrate the utility of these dually functionalized chitin nanocrystals, the bioaffinity of the resulting functionalized nanocrystals were confirmed by their interactions with the corresponding cognate proteins. The fluorescent label facilitates the observation of these interactions by either fluorescence imaging or even with the naked eye. Furthermore, the functionalized chitin nanocrystals were successfully applied to image *E. coli* by taking advantage of the affinity of the glyconanocrystals with the lectin receptor on the bacteria surface. Owing to the unique properties of chitin, such as biodegradability, biocompatibility, and nontoxicity, in comparison to many other nanomaterials, the new platform developed here may reveal opportunities for chitin-based nanomaterials in a wide range of bioanalytical and theranostic applications.

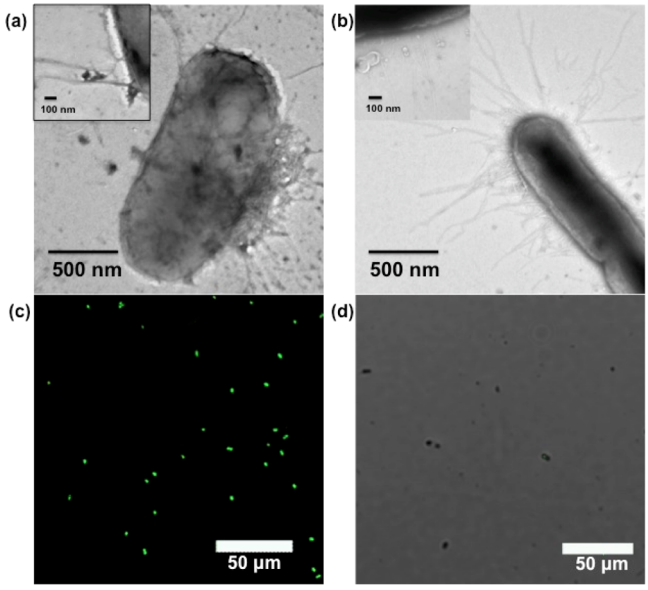

Figure 4. TEM images of TCN-dye-Man incubated with *E. coli* strains (a) ORN 178 and (b) ORN 208. (c,d) Corresponding confocal fluorescence microscopy images. The insets in (a) and (b) are the enlarged images of the corresponding samples.

■ ASSOCIATED CONTENT

Supporting Information

Synthesis, experimental details, and additional characterization data. This material is available free of charge via the Internet at http://pubs.acs.org.

■ AUTHOR INFORMATION

Corresponding Authors

*Phone: 978-934-3647. Fax: 978-934-3013. E-mail: mingdi_yan@uml.edu.

*Phone: 0046-08-7906915. Fax: 0046-08-7912333. E-mail: ramstrom@kth.se.

Author Contributions

The manuscript was written through contributions of all authors. All authors have given approval to the final version of the manuscript. Juan Zhou and Núria Butchosa contributed equally.

Notes

The authors declare no competing financial interest.

■ ACKNOWLEDGMENTS

The study was in part supported by the Royal Institute of Technology, the National Institutes of Health (R01GM080295), National Science Foundation (CHE-1112436), and the Swedish Research Council Formas (CarboMat, 2009-1687). J.Z. thanks the China Scholarship Council for a special scholarship award. The authors thank Professor Paul E. Orndorff (North Carolina State University) for providing *E. coli* strains ORN178 and ORN208.

REFERENCES

(1) Zeng, J., He, Y., Li, S., and Wang, Y. (2011) Chitin whiskers: an overview. *Biomacromolecules 13*, 1−11.

(2) Rejinold, N. S., Chennazhi, K. P., Tamura, H., Nair, S. V., and Rangasamy, J. (2011) Multifunctional chitin nanogels for simultaneous drug delivery, bioimaging, and biosensing. *ACS Appl. Mater. Interfaces 3*, 3654−3665.

(3) Lin, N., Huang, J., and Dufresne, A. (2012) Preparation, properties and applications of polysaccharide nanocrystals in advanced functional nanomaterials: a review. *Nanoscale 4*, 3274−3294.

(4) Pillai, C. K. S., Paul, W., and Sharma, C. P. (2009) Chitin and chitosan polymers: chemistry, solubility and fiber formation. *Prog. Polym. Sci. 34*, 641−678.

(5) Kurita, K. (2006) Chitin and chitosan: functional biopolymers from marine crustaceans. *Mar. Biotechnol. 8*, 203−226.

(6) Bhatnagar, A., and Sillanpaa, M. (2009) Applications of chitin- and chitosan-derivatives for the detoxification of water and wastewater - A short review. *Adv. Colloid Interface Sci. 152*, 26−38.

(7) Jenkins, D. W., and Hudson, S. M. (2001) Review of vinyl graft copolymerization featuring recent advances toward controlled radical-based reactions and illustrated with chitin/chitosan trunk polymers. *Chem. Rev. 101*, 3245−3274.

(8) Goodrich, J. D., and Winter, W. T. (2007) Alpha-Chitin nanocrystals prepared from shrimp shells and their specific surface area measurement. *Biomacromolecules 8*, 252−257.

(9) Fan, Y., Saito, T., and Isogai, A. (2008) Chitin nanocrystals prepared by TEMPO-mediated oxidation of alpha-chitin. *Biomacromolecules 9*, 192−198.

(10) Morin, A., and Dufresne, A. (2002) Nanocomposites of chitin whiskers from Riftia tubes and poly(caprolactone). *Macromolecules 35*, 2190−2199.

(11) Dong, S., and Roman, M. (2007) Fluorescently labeled cellulose nanocrystals for bioimaging applications. *J. Am. Chem. Soc. 129*, 13810−13811.

(12) Suginta, W., Khunkaewla, P., and Schulte, A. (2013) Electrochemical biosensor applications of polysaccharides chitin and chitosan. *Chem. Rev. 113*, 5458−5479.

(13) Beignet, J., Tiernan, J., Woo, C. H., Kariuki, B. M., and Cox, L. R. (2004) Stereoselective synthesis of allyl-C-mannosyl compounds: use of a temporary silicon connection in intramolecular allylation strategies with allylsilanes. *J. Org. Chem. 69*, 6341−6356.

(14) Deng, L., Norberg, O., Uppalapati, S., Yan, M., and Ramström, O. (2011) Stereoselective synthesis of light-activatable perfluorophenylazide-conjugated carbohydrates for glycoarray fabrication and evaluation of structural effects on protein binding by SPR imaging. *Org. Biomol. Chem. 9*, 3188−3198.

(15) Grayshan, P. H., Mak, K. H. R., and Peters, A. T. (1973) Heterocyclic derivatives of naphthalene-1, 8-dicarboxylic anhydride. Part II. Colour and dyeing properties on synthetic fibres of some substituted 7*H*-benzimidazo[2,1-*a*]benz[*de*]isoquinolin-7-ones. *J. Heterocyclic Chem. 10*, 705−710.

(16) Nakaya, K., Tanaka, T., Shirataki, Y., Shiozaki, H., Funabiki, K., Shibata, K., and Matsui, M. (2001) 4-(2-Aminoethylamino)-7H-benz[de]imidazo[2,1-a]isoquinolin-7-ones as a highly sensitive fluorescent labeling reagent for carnitine. *Bull. Chem. Soc. Jpn. 74*, 173−177.

(17) Lis, H., and Sharon, N. (1998) Lectins: carbohydrate-specific proteins that mediate cellular recognition. *Chem. Rev. 98*, 637−674.

(18) Kitano, H., Sumi, Y., and Tagawa, K. (2000) Recognition of novel lipopolypeptides with many pendent sugar residues by lectin. *Bioconjugate Chem. 12*, 56−61.

(19) Hardman, K. D., and Ainsworth, C. F. (1972) Structure of concanavalin A at 2, 4-Ang resolution. *Biochemistry 11*, 4910−4919.

(20) Lim, K. R., Ahn, K.-S., and Lee, W. (2013) Detection of concanavalin A based on attenuated fluorescence resonance energy transfer between quantum dots and mannose-stabilized gold nanoparticles. *Anal. Methods 5*, 64−67.

(21) Manimala, J. C., Roach, T. A., Li, Z. T., and Gildersleeve, J. C. (2006) High-throughput carbohydrate microarray analysis of 24 lectins. *Angew. Chem., Int. Ed. 45*, 3607−3610.

(22) Wang, X., Ramström, O., and Yan, M. (2011) Dye-doped silica nanoparticles as efficient labels for glycans. *Chem. Commun. 47*, 4261−4263.

(23) Wang, X., Ramström, O., and Yan, M. (2009) A photochemically initiated chemistry for coupling underivatized carbohydrates to gold nanoparticles. *J. Mater. Chem. 19*, 8944−8949.

(24) Lotan, R., Siegelman, H. W., Lis, H., and Sharon, N. (1974) Subunit structure of soybean agglutinin. *J. Biol. Chem. 249*, 1219−1224.

(25) Gordon, S., and Wood, M. (2009) Soybean agglutinin binding to corneal endothelial cell surfaces disrupts in situ monolayer integrity and actin organization and interferes with wound repair. *Cell Tissue Res. 335*, 551−563.

(26) Godula, K., and Bertozzi, C. R. (2012) Density variant glycan microarray for evaluating cross-linking of mucin-like glycoconjugates by lectins. *J. Am. Chem. Soc. 134*, 15732−15742.

(27) Kim, I. B., Wilson, J. N., and Bunz, U. H. F. (2005) Mannose-substituted PPEs detect lectins: A model for Ricin sensing. *Chem. Commun. 10*, 1273−1275.

(28) Phillips, R. L., Kim, I. B., Tolbert, L. M., and Bunz, U. H. F. (2008) Fluorescence self-quenching of a mannosylated poly(p-phenyleneethynylene) induced by Concanavalin A. *J. Am. Chem. Soc. 130*, 6952−6954.

(29) Swamy, M. J., Krishna Sastry, M. V., Khan, M. I., and Surolia, A. (1986) Thermodynamic and kinetic studies on saccharide binding to soya-bean agglutinin. *Biochem. J. 234*, 515−522.

(30) Mandal, D. K., Kishore, N., and Brewer, C. F. (1994) Thermodynamics of lectin-Carbohydrate interactions-titration microcalorimetry measurements of the binding of N-linked carbohydrates and ovalbumin to Concanavalin A. *Biochemistry 33*, 1149−1156.

(31) Norberg, O., Deng, L., Aastrup, T., Yan, M., and Ramström, O. (2010) Photo-click immobilization on quartz crystal microbalance sensors for selective carbohydrate-protein interaction analyses. *Anal. Chem. 83*, 1000−1007.

(32) Harris, S. L., Spears, P. A., Havell, E. A., Hamrick, T. S., Horton, J. R., and Orndorff, P. E. (2001) Characterization of escherichia colitype 1 pilus mutants with altered binding specificities. *J. Bacteriol. 183*, 4099−4102.

(33) Liu, L., Dietsch, H., Schurtenberger, P., and Yan, M. (2009) Photoinitiated coupling of unmodified monosaccharides to iron oxide nanoparticles for sensing proteins and bacteria. *Bioconjugate Chem. 20*, 1349−1355.

(34) Phillips, R. L., Kim, I. B., Carson, B. E., Tidberk, B., Lowary, T. L., Tolbert, L. M., and Bunz, U. H. F. (2008) Sugar-substituted poly(p-phenyleneethynylene)s: sensitivity enhancement toward lectins and bacteria. *Macromolecules 41*, 7316−7320.